Development 140, 31-42 (2013) doi:10.1242/dev.081851

MEF2A regulates the *Gtl2-Dio3* microRNA mega-cluster to modulate WNT signaling in skeletal muscle regeneration

Christine M. Snyder[1], Amanda L. Rice[1,*], Nelsa L. Estrella[1,*], Aaron Held[1], Susan C. Kandarian[2] and Francisco J. Naya[1,‡]

SUMMARY

Understanding the molecular mechanisms of skeletal muscle regeneration is crucial to exploiting this pathway for use in tissue repair. Our data demonstrate that the MEF2A transcription factor plays an essential role in skeletal muscle regeneration in adult mice. Injured *Mef2a* knockout mice display widespread necrosis and impaired myofiber formation. MEF2A controls this process through its direct regulation of the largest known mammalian microRNA (miRNA) cluster, the *Gtl2-Dio3* locus. A subset of the *Gtl2-Dio3* miRNAs represses secreted Frizzled-related proteins (sFRPs), inhibitors of WNT signaling. Consistent with these data, *Gtl2-Dio3*-encoded miRNAs are downregulated in regenerating *Mef2a* knockout muscle, resulting in upregulated sFRP expression and attenuated WNT activity. Furthermore, myogenic differentiation in *Mef2a*-deficient myoblasts is rescued by overexpression of miR-410 and miR-433, two miRNAs in the *Gtl2-Dio3* locus that repress sFRP2, or by treatment with recombinant WNT3A and WNT5A. Thus, miRNA-mediated modulation of WNT signaling by MEF2A is a requisite step for proper muscle regeneration, and represents an attractive pathway for enhancing regeneration of diseased muscle.

KEY WORDS: MEF2, Muscle regeneration, miRNA, Mouse

INTRODUCTION

Skeletal muscle has the ability to regenerate myofibers upon damage or disease. The muscle repair process involves activation of quiescent muscle stem cells, called satellite cells, which proliferate and subsequently enter the differentiation pathway leading to the formation of multi-nucleated myotubes (Shi and Garry, 2006; Kuang and Rudnicki, 2008; Tedesco et al., 2010). Genetic dissection of this process has revealed that developmental pathways required for embryonic myogenesis also regulate muscle regeneration (Parker et al., 2003; Chargé and Rudnicki, 2004; Tajbakhsh, 2009). For example, the WNT signaling transduction cascade provides positional cues that establish myogenic identity within the developing somite (Buckingham, 2006). This pathway is later deployed to regulate the differentiation of activated satellite cells in response to injury (Polesskaya et al., 2003; Brack et al., 2008). Likewise, the paired homeobox transcription factor PAX7 plays a crucial role in progenitor cells in embryonic myogenesis and early postnatal skeletal muscle regeneration (Kuang et al., 2006; Buckingham and Relaix, 2007; Lepper et al., 2009).

Myocyte enhancer factor 2 (MEF2), an evolutionarily conserved transcription factor, is required for the differentiation of all three muscle lineages in flies (Bour et al., 1995; Lilly et al., 1995). In mammals, which have four *Mef2* genes, an unequivocal role for MEF2 in muscle differentiation *in vivo* has yet to be established. The lack of an overt muscle differentiation defect is likely to be due to functionally redundant MEF2-dependent gene regulatory mechanisms (Black and Olson, 1998; Potthoff and Olson, 2007). Nevertheless, MEF2 loss-of-function analysis in mice has revealed distinct roles for individual family members in skeletal muscle. Developing myoblasts in mice lacking MEF2C are able to differentiate, but the resulting skeletal myofibers display disorganized cytoarchitecture (Potthoff et al., 2007a). MEF2C and MEF2D are also required for the formation of specialized skeletal muscle fiber types (Potthoff et al., 2007b). Despite the finding that inactivating mutations in some MEF2 family members in mice result in specific perturbations in skeletal muscle, a detailed understanding of MEF2 function in this tissue is far from complete.

MicroRNAs (miRNAs) are small, non-coding RNAs which function post-transcriptionally by interacting directly with mRNAs to repress their expression (Bartel, 2004). All cell types express miRNAs but a subset exhibit restricted expression, such as the muscle-specific miRNAs miR-1 and miR-133 (Lagos-Quintana et al., 2002; Chen et al., 2006; Liu et al., 2007). These and other more broadly expressed miRNAs have been shown to play important modulatory roles in a variety of skeletal muscle processes (van Rooij et al., 2008; Chen et al., 2009). However, only a limited number of miRNAs have been linked to the regulation of skeletal muscle regeneration. miR-1 and miR-206 have been shown to control PAX7 levels in satellite cell proliferation and differentiation (Chen et al., 2010), whereas miR-27b regulates PAX3 expression in this process (Crist et al., 2009). As the balance between proliferation and differentiation of progenitor cells in muscle regeneration must be carefully orchestrated, it is likely that additional miRNAs exist that modulate this process.

In the present study we explored the function of MEF2A in skeletal muscle. We report that, contrary to skeletal muscle development, MEF2A is required for adult myogenesis in response to injury. Skeletal muscle injury in adult *Mef2a* knockout mice resulted in widespread necrosis and attenuated myofiber regeneration accompanied by a significant reduction in PAX7-positive (PAX7+) nuclei. This impaired injury response was associated with a downregulation of the largest known mammalian miRNA cluster, the *Gtl2-Dio3* locus, harboring >40 miRNAs. A cohort of these miRNAs directly targets secreted Frizzled-related

[1]Department of Biology, Program in Cell and Molecular Biology and [2]Department of Health Sciences, Boston University, Boston, MA 02215, USA.

*These authors contributed equally to this work
‡Author for correspondence (fnaya@bu.edu)

Accepted 3 October 2012

protein 2 (sFRP2), an inhibitor of the WNT signaling pathway. Accordingly, we detected an upregulation of sFRP2 in regenerating *Mef2a* knockout skeletal muscle along with reduced WNT activity. Finally, overexpression of miRNAs that directly repress sFRP2 or addition of recombinant WNTs was able to rescue myogenic differentiation in *Mef2a*-deficient myoblasts.

MATERIALS AND METHODS

Cell culture

C2C12 and COS cells were cultured as described previously (McCalmon et al., 2010). For differentiation assays, C2C12 cells were switched to DMEM supplemented with 2% horse serum (differentiation media) 24 hours post-transfection/transduction. Primary skeletal myoblasts and single myofibers were isolated and cultured from uninjured or cardiotoxin-injured adult mouse hindlimb muscle as described by Springer et al. (Springer et al., 1997).

Plasmids and miRNA mimics

MEF2A-FLAG and MEF2C-FLAG plasmids were generated by cloning full-length mouse cDNAs into pCMV-tag4 (Invitrogen). MEF2B-FLAG and MEF2D-FLAG (human) were kind gifts of T. Gulick (Sanford Burnham Medical Research Institute, Orlando, FL, USA). The mouse *Gtl2* promoter (0.5 kb) containing the MEF2 binding site was cloned into pGL3-Basic (Promega). The mutant *Gtl2* reporter was generated by mutating the –39 MEF2 site CTT to GGG, without altering the overlapping TATA box (–39MUT). For 3′UTR reporter assays, the 3′UTR (892 bp) of mouse sFRP2 was cloned into pMIR-REPORT (Ambion). The mutant 3′UTR-sFRP2 construct was generated by mutating the miR-410 seed sequence binding site TTATAT to GGGGGG. pMIR-REPORT-β-galactosidase (Ambion), pCMV-*Renilla*-luciferase and pTOPFLASH (Addgene) were also used for luciferase assays. MiRNA mimics were purchased from Ambion.

Short hairpin RNA (shRNA) design and knockdown in C2C12 cells

Adenoviruses carrying shRNAs specific for *Mef2a* or *lacZ* were generated as described previously (Ewen et al., 2011). Adenoviruses were used at a multiplicity of infection (MOI) of 25 for all assays.

Muscle injury and histology

Tibialis anterior (TA) muscle of wild-type (WT) and *Mef2a* knockout (KO) mice (Naya et al., 2002) were injected with 10 μM cardiotoxin (*Naja nigricollis*, EMD chemicals) and harvested several days post-injury. Transverse muscle sections were stained with Hematoxylin and Eosin for visualization of basic muscle morphology.

Cell culture immunofluorescence and TUNEL assays

Phase contrast images of C2C12 DIFF 3 cells (post-transduction) were taken using an Olympus MX50 microscope. For immunofluorescence, primary antibodies included: anti-α-actinin (1:200; Sigma), anti-Pax7 [1:2; supernatant, Developmental Studies Hybridoma Bank (DSHB)], anti-MEF2 (1:200; Santa Cruz Biotechnology) and anti-MyoD (1:200 S-17, 1:100 M-318; Santa Cruz Biotechnology). Secondary antibodies were: anti-mouse Alexa Fluor 488, 568 IgG1 and 568 IgG (H+L) (1:300); anti-rabbit Alexa Fluor 488 and 568 (1:300); and anti-goat Alexa Fluor 647 (1:100) (Invitrogen). Terminal dUTP nick-end labeling (TUNEL) assays were performed using the Promega DeadEnd Fluorometric TUNEL System Kit. Vectashield mounting medium with DAPI was applied to all slides. Fluorescent images were taken using an Olympus DSU Spinning Disk Confocal microscope.

Immunohistochemistry

Transverse TA muscle cryosections (10 μm) were immunostained as described in Kanisicak et al. (Kanisicak et al., 2009). Primary antibodies were: anti-laminin (1:200; Sigma), anti-β-catenin (1:200, BD Transduction Labs), anti-Pax7 and anti-MEF2. Secondary antibodies were: anti-mouse Alexa-Fluor 488 IgG (H+L), anti-mouse Alexa-Fluor 568 IgG_1, and fluorescein anti-rabbit IgG (H+L) (1:500; Vector Labs). Cross-sectional area (CSA) of skeletal muscle was assessed by Metamorph (Molecular Devices, Downington, PA, USA) analysis of laminin-stained muscle sections.

Microarray

Total RNA from WT (n=5) and *Mef2a* KO (n=5) TA muscle 7 days post-injury was prepared by TRIZOL isolation (Invitrogen), and were hybridized to the Mouse Gene 1.0 ST Array (Affymetrix) at the Boston University Microarray Facility. Microarray data are available in GEO with Accession Number GSE41871.

RT-PCR and qRT-PCR/stem-loop qRT-PCR

Pooled RNA from TA muscle or C2C12 MEF2A knockdown experiments (n=6) was used to synthesize cDNA using reverse transcriptase (M-MLV) with random hexamers according to the manufacturer's instructions (Promega). cDNAs were synthesized using the TaqMan miRNA Reverse Transcriptase Kit (Applied Biosystems) for detection of mature miRNAs *in vivo* as described by Chen et al. (Chen et al., 2005). miRNA and 5S sequences were amplified using forward-specific primers and a universal reverse primer (Thompson et al., 2011). Quantitative RT-PCR was performed in triplicate wells using Power SYBR Green Master Mix (Applied Biosystems) with the 7900HT Sequence Detection System (Applied Biosystems). Primers used for all RT-PCR and qRT-PCR/stem-loop qRT-PCR analyses are listed in supplementary material Table S1.

Luciferase assays

Luciferase assays were performed using Luciferase Assay Reagent (LAR, Promega), and results were normalized by β-galactosidase assay (Miller, 1972). miRNA mimics and expression plasmids were transfected using the RNAiMAX transfection reagent (Invitrogen). TOPFLASH assays were performed on C2C12 cells at DIFF 3 using LARII (Promega) and normalized by *Renilla* luciferase assay (Promega). All luciferase assays were performed in triplicate (n>3).

Western blot analysis

Western blots were performed as previously described (McCalmon et al., 2010). Antibodies included: anti-GAPDH (1:5000; Santa Cruz), anti-MEF2A (1:1000), anti-cleaved-caspase-3 (1:1000; Cell Signaling), anti-FLAG (1:10,000; Sigma), anti-sFRP2 (1:500; Millipore), anti-MF 20 (1:50; supernatant, DSHB) and anti-β-catenin (1:1000). Blots were incubated with horseradish peroxidase-conjugated secondary antibodies (1:10,000; Sigma) and reacted with Western Lightning Chemiluminescent Reagent (Perkin Elmer).

Electrophoretic mobility shift assays

In vitro-translated mouse MEF2A (rabbit reticulocyte lysate; Promega) or nuclear extracts from C2C12 myotubes were used for gel shift assays. The mutant MEF2 site was generated in the same manner as the mutant *Gtl2* reporter. Supershift assays were performed with anti-MEF2 antibodies (C-21, Santa Cruz). Competitions were performed with 100-fold molar excess of unlabeled probe. Gel shift reactions were fractionated on 5% non-denaturing polyacrylamide gels, dried, and exposed to a phosphor-imaging screen (Amersham Biosciences).

Chromatin immunoprecipitation

Chromatin was immunoprecipitated from C2C12 cells (DIFF 3) transfected with mouse MEF2A (pcDNA3-MEF2A-FLAG) using the anti-FLAG (Sigma) antibody, or negative control anti-HA antibody (Sigma). Chromatin was subjected to qRT-PCR for the detection of the *Gtl2* promoter sequence containing the –39 MEF2 site. Primer sequences are listed in supplementary material Table S1.

miRNA rescue assay and miR knockdown

For rescue experiments, C2C12 myoblasts were transduced with adenoviruses (sh*lacZ* or sh*Mef2a*) at MOI 25 and transfected with 40 nM miRNA mimics (miR negative control #1, miR-410, miR-433, or an equimolar combination) 24 hours post-transduction. For miR knockdown experiments, C2C12 myoblasts were transfected with 100 pmol anti-miR-410 or anti-miR-433 (Ambion) using RNAi Max (Invitrogen). Cells were then differentiated in culture for three days prior to imaging or RNA/protein analysis.

WNT rescue assay

C2C12 myoblasts were transduced with adenoviruses (sh*lacZ* or sh*Mef2a*) at MOI 25 and recombinant WNTs were added 24 hours post-transduction.

recombinant mouse WNT3A (rmWnt3a) was used at 100 ng/ml and recombinant human/mouse WNT5A (rh/mWnt5a) was used at 200 ng/ml (R&D Systems). For combinatorial rescue, WNT concentrations were halved. Cells were imaged on differentiation day three.

Statistical analysis

All numerical quantification is representative of the mean±s.e.m. of at least three independently performed experiments. Statistically significant differences between two populations of data were determined using Student's *t*-test. *P*-values of ≤0.05 were considered to be statistically significant.

RESULTS

MEF2A knockdown in C2C12 myoblasts results in impaired myotube formation

To dissect the role of MEF2A in skeletal muscle differentiation, C2C12 cells were transduced at various time points with adenovirus harboring a *Mef2a*-specific shRNA (sh*Mef2a*), which effectively knocked down MEF2A expression (Ewen et al., 2011) (supplementary material Fig. S1A). As shown in Fig. 1A, knockdown of MEF2A in proliferating C2C12 myoblasts (DIFF –1) resulted in severely compromised myotube formation by differentiation day three (DIFF 3). Knockdown of MEF2A in differentiated C2C12 cells (DIFF 3 and DIFF 7) also caused substantial loss of myotubes (Fig. 1A). Immunofluorescence analysis of *Mef2a*-deficient C2C12 cells at day three revealed a 46% reduction in differentiation (Fig. 1B) and a 49% decrease in myoblast fusion (Fig. 1B). The reduction in myotube number resulted, in part, from programmed cell death as shown by a 1.5-fold increase in TUNEL-positive cells (Fig. 1C) and increased expression of activated caspase-3 (Fig. 1D).

Collectively, the results of the C2C12 knockdown experiments revealed that MEF2A is essential for myogenic differentiation. This differentiation defect is in stark contrast to *Mef2a* knockout (KO) mice which do not display developmental skeletal muscle abnormalities (Potthoff et al., 2007b). The phenotypic differences may be explained, in part, by the radically different *Mef2* temporal expression in C2C12 cells compared with that observed during

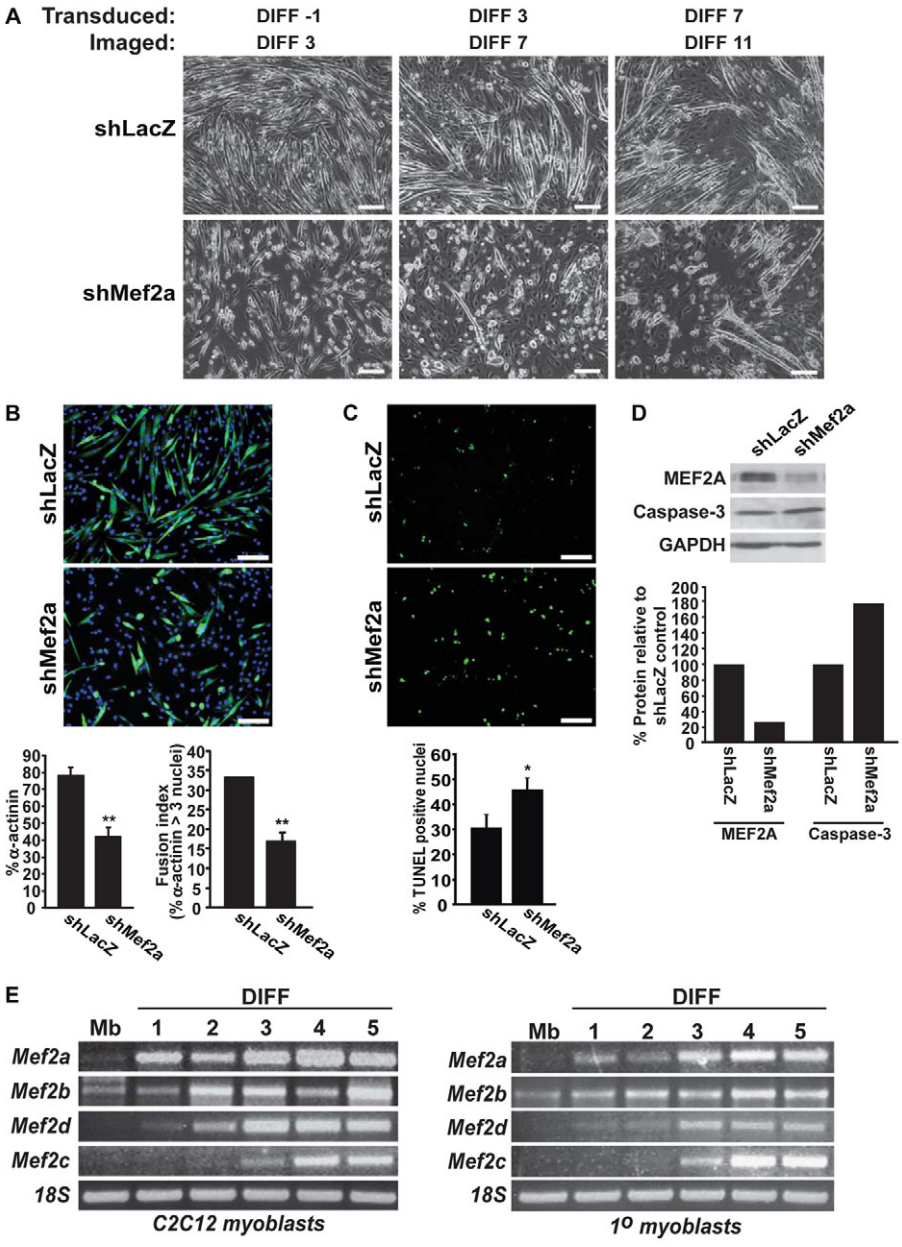

Fig. 1. MEF2A knockdown inhibits muscle differentiation. (**A**) Phase contrast images of differentiated C2C12 cells transduced with either sh*lacZ* or sh*Mef2a* adenovirus. Time points at which cells were transduced and subsequently imaged are indicated. DIFF –1 indicates subconfluent proliferating myoblasts. (**B**) C2C12 immunofluorescence with the differentiation marker α-actinin (green) and nuclear stain DAPI (blue) at DIFF 3. Differentiation (lower left graph) and fusion (lower right graph) indices were quantified as the percentage of nuclei present in α-actinin-positive cells and α-actinin-positive cells containing three or more nuclei, respectively (*n*=3). (**C**) C2C12 DIFF 3 fluorescent TUNEL stain. Apoptotic index was calculated as the percent TUNEL-positive nuclei (green) relative to total nuclei (*n*=3). (**D**) Immunoblot of activated, cleaved-caspase-3 expression to assess extent of apoptosis. Quantification of immunoblot reveals an increase in activated, cleaved-caspase-3 in sh*Mef2a*-transduced C2C12 cells. Band density was calculated as a percentage of the sh*lacZ* control. (**E**) RT-PCR expression analysis of the *Mef2* family during differentiation in C2C12 and primary myoblasts from injured muscle. MB, myoblasts; DIFF, differentiation day. Error bars represent s.e.m. **P*<0.05, ***P*<0.01. Scale bars: 100 μm.

muscle development (Edmondson et al., 1994). Contrary to embryonic myogenesis, in which *Mef2c* is expressed first, in C2C12 cells *Mef2a* is expressed earlier than *Mef2c* and in proliferating myoblasts (Mbs) (Fig. 1E). Expression of *Mef2a* is subsequently upregulated upon induction of myogenic differentiation and this higher expression is maintained throughout myotube differentiation and maturation. In C2C12 cells, *Mef2d* and *Mef2c* are expressed one and two days after *Mef2a*, respectively. *Mef2b* is also expressed in proliferating myoblasts but its levels remain constant throughout differentiation. As C2C12 myoblasts were originally isolated from injured muscle (Yaffe and Saxel, 1977; Blau et al., 1983), these results suggest that the C2C12 differentiation process might reflect muscle regeneration. To test this notion, we isolated primary myoblasts from injured muscle and analyzed *Mef2* temporal expression. Indeed, the pattern of *Mef2* expression in proliferating and differentiated primary myoblasts was similar to that observed in C2C12 cells (Fig. 1E; supplementary material Fig. S1D and Fig. S2). Thus, we postulate that *Mef2* regulation is reprogrammed during regeneration and that the pronounced defect in C2C12 differentiation reflects a specialized function for MEF2A in skeletal muscle regeneration.

Mef2a knockout mice display impaired regenerative myogenesis

To determine whether MEF2A plays a role in skeletal muscle regeneration, we induced muscle injury in adult *Mef2a* KO mice (129Sv/C57Bl6 mixed genetic background) by injecting the tibialis anterior (TA) muscle with cardiotoxin. TA muscle from *Mef2a* KO mice displayed widespread necrosis at various time points after injury compared with wild-type (WT) animals (Fig. 2A). Transverse muscle sections revealed a similar extent of damage in both WT and KO tissue at day 3 (Fig. 2B). However, by day 7, unlike WT muscle, *Mef2a* KO muscle displayed an intense basophilic appearance, consistent with the presence of necrotic tissue (Fig. 2B). By day 14, necrosis was diminished in *Mef2a* KO muscle and these areas were replaced by regenerating myofibers (Fig. 2B). By day 21, abundant regenerating myofibers were clearly evident and necrosis was largely absent (supplementary material Fig. S1E), suggesting a delay, but not a block, in regeneration.

To characterize this impaired regenerative response in greater detail, cross-sectional area (CSA) of non-necrotic myofibers possessing centrally located nuclei, a hallmark of regenerating myofibers, was measured in TA muscle. Metamorph analysis at day 7 of TA muscle sections immunostained with anti-laminin revealed significantly reduced CSA of regenerating *Mef2a* KO tissue (Fig. 2C). By day 14, *Mef2a* KO muscle displayed a slight increase in CSA relative to earlier time points, but not to the extent observed in WT muscle (Fig. 2C), supporting the notion that muscle regeneration is delayed but not blocked in these mice.

As global *Mef2a* KO mice were used for this study, we wanted to determine next whether impaired muscle regeneration could be attributable to a specific defect in myoblasts. For this characterization, we isolated primary myoblasts from injured WT and KO muscle and induced them to differentiate in culture. As shown in Fig. 3A, *Mef2a* KO myoblasts were unable to differentiate effectively, as demonstrated by a 78% reduction in α-actinin staining. Moreover, there was no significant difference in cell proliferation and viability (data not shown) or in MyoD-positive myoblasts (Fig. 3A), demonstrating that *Mef2a* KO myoblasts are appropriately specified and have committed to the myogenic pathway.

The defect in myogenic differentiation *in vitro* prompted us to analyze injured *Mef2a* KO muscle in greater detail using the muscle satellite cell marker PAX7 as a perturbation in the PAX7+ progenitor population and/or its expression is one reliable indicator of myogenic impairment. At day 7 post-injury, there was a 50% reduction in the number of PAX7+ nuclei colocalized with DAPI in regenerating *Mef2a* KO muscle compared with regenerating WT muscle (Fig. 3B). However, uninjured *Mef2a* KO muscle displayed a similar number of quiescent PAX7+/DAPI nuclei compared with uninjured WT muscle (data not shown) indicating that the reduction in the PAX7+ progenitor population is only observed in a muscle injury setting. PAX7 transcripts were also significantly downregulated in both regenerating *Mef2a* KO muscle and in primary myoblasts isolated from these injured mice (Fig. 3C). These results indicate that impaired regeneration in *Mef2a* KO muscle is, in part, due to defective muscle differentiation and suggest that loss of MEF2A affects the ability of injured muscle to generate (or maintain) sufficient activated satellite cells for subsequent myotube formation.

A mega-cluster of microRNAs is downregulated in regenerating *Mef2a* KO muscle

To dissect the molecular mechanisms of this defective muscle regeneration, we isolated RNA from WT and *Mef2a* KO injured TA muscle and performed microarray analysis. The most striking result of this analysis was the downregulation of >40 microRNAs (miRNAs) (Fig. 4A; supplementary material Table S2). Further characterization revealed that these miRNAs all localize to a single locus on mouse chromosome 12 (Fig. 4B). This locus is known as the *Gtl2-Dio3* domain and is the largest known miRNA cluster in the mammalian genome (Seitz et al., 2004; Kircher et al., 2008).

To confirm the microarray data, we examined the expression of coding and non-coding transcripts in the *Gtl2-Dio3* locus. Expression of the upstream *Dlk1* gene, which has been shown to play a role in skeletal muscle development and regeneration (Waddell et al., 2010), was unaffected in regenerating *Mef2a* KO muscle (Fig. 4C). By contrast, analysis of selected miRNA transcripts in the *Gtl2-Dio3* locus, which were retrospectively chosen based on their common target mRNAs (see Fig. 5A), displayed significant downregulation in this tissue (Fig. 4C), in primary KO myoblasts (supplementary material Fig. S3E-I) and in *Mef2a*-deficient C2C12 cells (Fig. 4D). We also determined that these miRNAs are upregulated in WT primary myoblast and C2C12 differentiation (supplementary material Fig. S3D-I), paralleling the expression profile of MEF2A (supplementary material Fig. S3B,C). Furthermore, our tissue expression profiling revealed that, in addition to the brain (Seitz et al., 2004; Schratt et al., 2006), *Gtl2-Dio3* miRNAs are enriched in skeletal muscle and the heart (supplementary material Fig. S3A). These data strongly suggest that MEF2A regulates the expression of *Gtl2-Dio3* miRNAs.

MEF2A directly regulates the *Gtl2* promoter upstream of all miRNAs in the cluster

Previous studies have shown that the miRNAs in the *Gtl2-Dio3* cluster are coordinately misregulated in mouse models harboring mutations that affect expression of this locus (Lin et al., 2003; Zhou et al., 2010). Because all miRNAs in the *Gtl2-Dio3* locus are downregulated in regenerating *Mef2a* KO muscle, we hypothesized that transcription of this cluster may be controlled by MEF2A through an upstream *cis*-acting sequence.

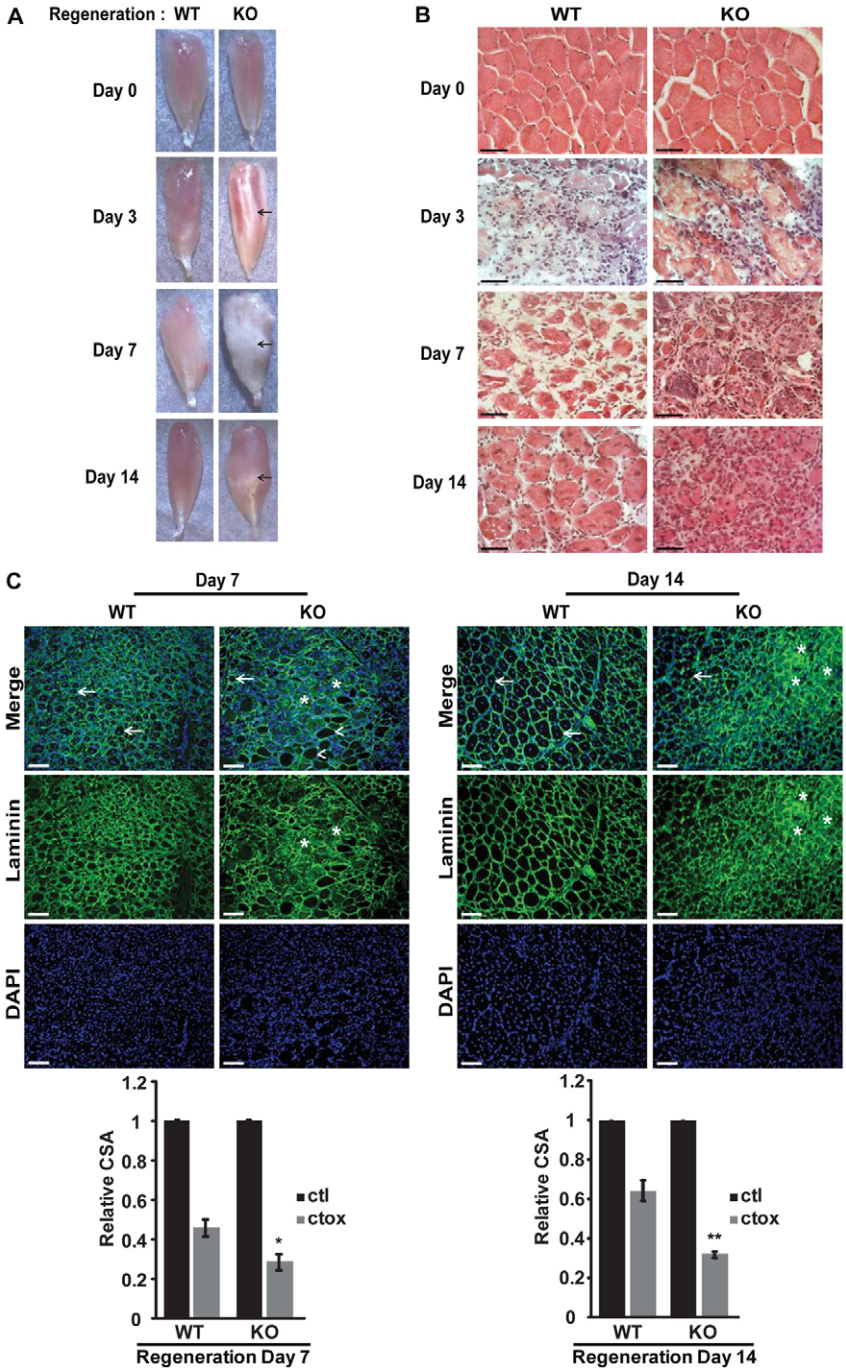

Fig. 2. *Mef2a* KO mice exhibit impaired regenerative myogenesis. (**A**) Images of whole tibialis anterior (TA) muscle from adult wild-type (WT) and *Mef2a* KO (KO) mice post-cardiotoxin-induced injury; necrotic areas are indicated (arrows). (**B**) Hematoxylin and Eosin staining of transverse TA muscle sections. WT and KO uninjured (day 0) and cardiotoxin-injured muscle at regeneration day 3, 7, and 14 are shown. Intense basophilic staining indicates necrosis (n=5). (**C**) Fluorescent laminin- (cell periphery) and DAPI-stained TA muscle, 7 and 14 days post-injury. Necrotic areas (asterisks), undamaged myofibers (arrowheads) and regenerating myofibers (arrows) are indicated. Cross sectional area (CSA) analysis of regenerating myofiber size for each ctox time point is shown relative to ctls normalized to 1 (n=5). CSA increases by 4% in KO muscle (0.28 to 0.32) from day 7 to day 14, whereas CSA of WT muscle increases by 19% (0.46 to 0.65). Error bars represent s.e.m. *P<0.05, **P<0.01. Black scale bars: 50 μm; white scale bars: 100 μm.

We identified a conserved MEF2 site located at position –39 upstream of the *Gtl2* transcription start site, which overlaps the only defined TATA box in the entire locus (Zhou et al., 2010). *In vitro* gel shift assays showed that MEF2A binds to this MEF2 site, which is effectively competed by the unlabeled oligonucleotide, but is unable to bind to a mutant probe harboring a specific mutation in the MEF2 sequence (Fig. 4E). Nuclear extracts from C2C12 myotubes incubated with the –39 MEF2 site showed robust DNA binding, and this complex was supershifted when incubated with a MEF2A antibody (Fig. 4E). To demonstrate that MEF2A associates with the *Gtl2* proximal promoter region *in vivo*, we subjected chromatin from C2C12 myotubes transfected with MEF2A-FLAG to chromatin immunoprecipitation assays. Incubation of these extracts with anti-FLAG showed highly enriched MEF2A binding to this region (Fig. 4F).

To determine whether the *Gtl2* promoter is active in muscle, we compared the activity of the proximal promoter in non-muscle COS cells and C2C12 myoblasts. Transfection of the *Gtl2* proximal promoter revealed a significantly higher activity in C2C12 myoblasts that was dependent on an intact MEF2 site (Fig. 4G). We next asked whether MEF2A could activate the *Gtl2* proximal promoter harboring the MEF2 site. COS cells co-transfected with MEF2A and the *Gtl2* promoter reporter resulted in a threefold higher level of activation compared with reporter alone (Fig. 4H). Mutation of the MEF2 site, without affecting the TATA element,

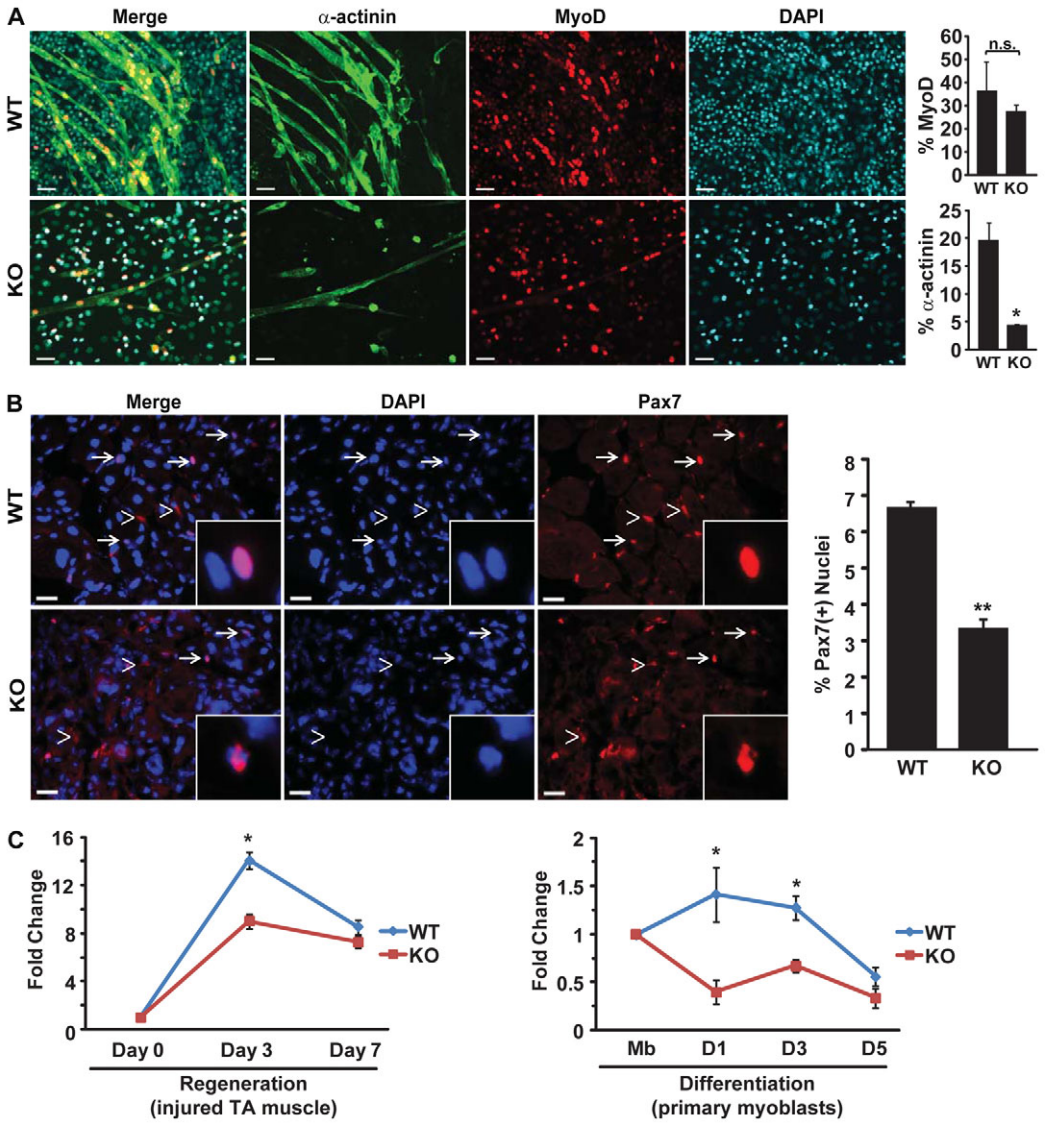

Fig. 3. Primary myoblasts from *Mef2a* KO are differentiation defective. (**A**) Immunofluorescence of α-actinin and MyoD in primary WT and KO myoblasts from adult injured muscle at DIFF 3. Myogenic commitment was calculated as the percentage of nuclei expressing MyoD (upper right graph) and differentiation as the percentage of nuclei present in α-actinin+ cells (lower right graph) (*n*=2). (**B**) Immunofluorescence of PAX7 in TA muscle, 7 days post-injury. Arrows indicate PAX7+ nuclei (red) colocalized with DAPI (blue). Arrowheads indicate PAX7 signal not colocalized with DAPI (non-specific). Quantification of the percentage of PAX7+ nuclei colocalized with DAPI is shown (*n*=3). (**C**) qRT-PCR analysis of *Pax7* expression *in vivo* (left, *n*=3) and in primary myoblasts (right, *n*=4) isolated from injured WT and KO muscle. Error bars represent s.e.m. **P*<0.05, ***P*<0.01. Scale bars: 20 μm.

resulted in a significant decrease in MEF2A-dependent transcriptional activation (Fig. 4H). The results above suggest that MEF2A directly regulates the *Gtl2-Dio3* cluster from the *Gtl2* proximal promoter region.

Gtl2-Dio3 miRNAs target WNT signaling inhibitors

To understand the mechanism by which MEF2A regulates skeletal muscle regeneration through this miRNA mega-cluster we subjected all miRNA sequences within the cluster to miRNA prediction algorithms (Target Scan and MirANDA). The results of these analyses revealed that many of the miRNAs in the *Gtl2-Dio3* mega-cluster are predicted to target secreted Frizzled-related proteins (sFRPs) 1, 2 and 4 (Fig. 5A), members of a well-known family of inhibitors in the WNT signaling pathway (Kawano and Kypta, 2003; MacDonald et al., 2009).

Given the results described above, we examined the expression levels of *Sfrp1*, *Sfrp2* and *Sfrp4* in regenerating WT and *Mef2a* KO muscle. We found that expression of *Sfrp1*, *Sfrp2* and *Sfrp4* was significantly upregulated (Fig. 5B) and that sFRP2 protein is upregulated in regenerating *Mef2a* KO muscle (Fig. 5C). We extended these results by examining the temporal expression of *Sfrp2* and selected *Gtl2-Dio3* miRNAs predicted to target *Sfrp2* in regeneration. As shown in Fig. 5D, between days one and three post-injury, when muscle is degenerating, the *Gtl2-Dio3* miRNAs were downregulated whereas *Sfrp2* was upregulated (Fig. 5D). At these early time points, we did not find any significant difference in expression of either the miRNAs or *Sfrp2* between WT and *Mef2a* KO muscle. Between days three and seven post-injury, when activated myoblasts begin forming nascent myofibers, miRNA expression increased in WT muscle approaching pre-injury

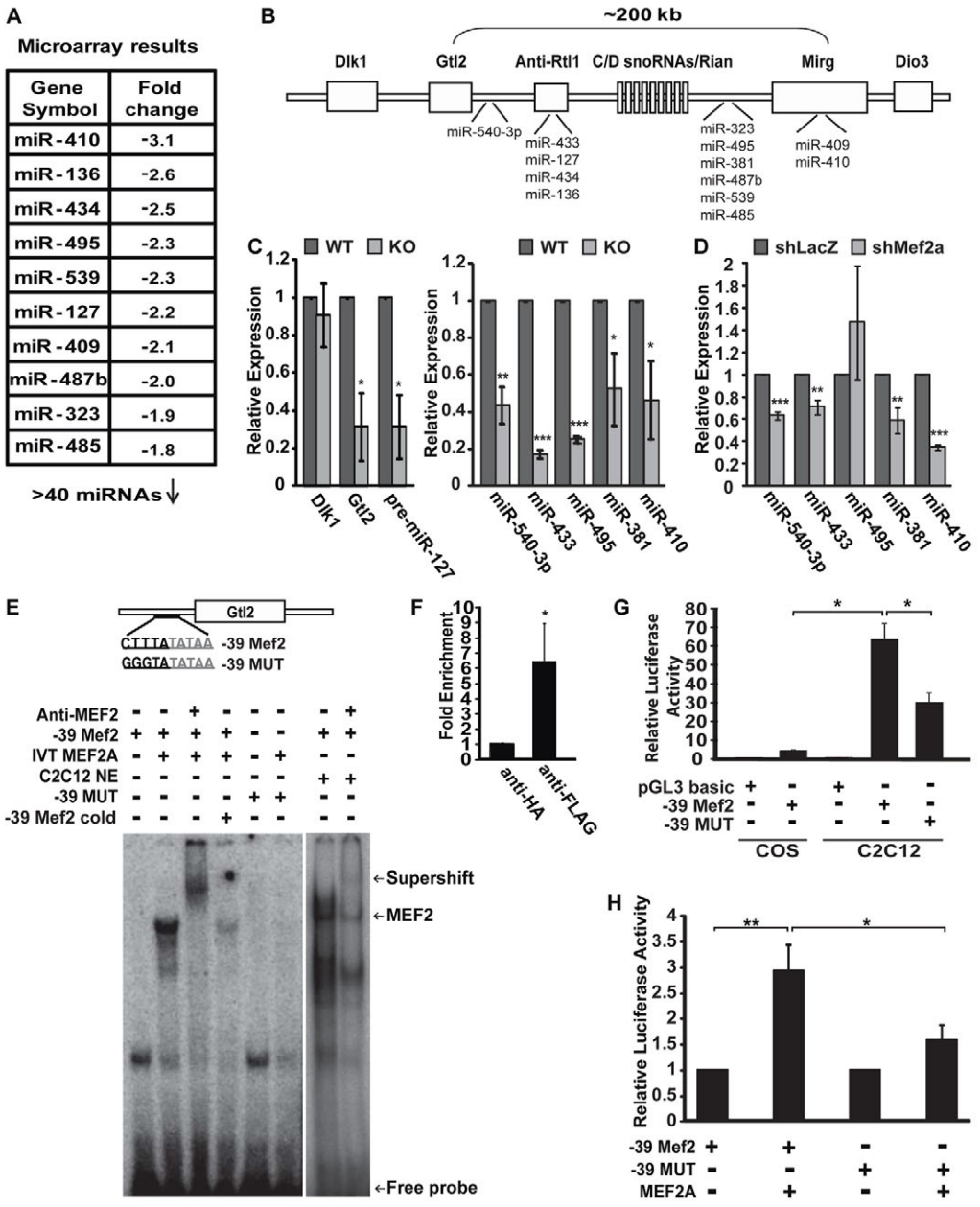

Fig. 4. The *Gtl2-Dio3* microRNA mega-cluster is directly regulated by MEF2A. (**A**) The top ten most downregulated miRNAs in injured TA muscle from *Mef2a* KO mice (n=5), 7 days post-injury, and their fold change in expression by microarray. More than 40 downregulated miRNAs, including the top ten, localize to the *Gtl2-Dio3* locus. (**B**) Depiction of the *Gtl2-Dio3* miRNA mega-cluster locus on mouse chromosome 12. Relative positions of the top downregulated miRNAs listed in A are shown. Several miRNAs not present in the table in A were retrospectively included because they are predicted to target *Sfrp2*. Grouped miRNAs, listed from top to bottom, reflects their 5′ to 3′ order within the *Gtl2-Dio3* locus. (**C**) *In vivo* qRT-PCR analysis of selected miRNA transcripts and those predicted to target *Sfrp2* within the *Gtl2-Dio3* locus in injured WT and KO samples (n=3). Expression is relative to WT normalized to 1. (**D**) *In vitro* qRT-PCR analysis of the miRNA transcripts described in C in C2C12 cells (DIFF 3) transduced with sh*lacZ* or sh*Mef2a* adenovirus. Expression is relative to sh*lacZ* normalized to 1. (**E**) Gel shift assay reveals binding of *in vitro* translated MEF2A to wild-type but not mutant –39 MEF2 site. Incubation with MEF2A antibodies shift the MEF2 complex bound to the –39 MEF2 probe. Binding of MEF2A to the –39 MEF2 site is competed by unlabeled probe. The –39 MEF2 site upstream of *Gtl2* is shown with the overlapping TATA box (gray). (**F**) Chromatin immunoprecipitation (ChIP) analysis of the *Gtl2* promoter region containing the –39 MEF2 site in MEF2A-FLAG immunoprecipitates compared with anti-HA (negative control) (n=5). (**G**) Luciferase analysis of the *Gtl2* promoter showing muscle-specific activation of the reporter (n=3). (**H**) Luciferase analysis of WT and MEF2 mutant *Gtl2* reporter activity in COS cells transfected with mouse MEF2A (n=5). Error bars represent s.e.m. *P<0.05, **P<0.01, ***P<0.001.

levels but failed to be upregulated in injured *Mef2a* KO muscle (Fig. 5D). In a reciprocal fashion, the expression of *Sfrp2* decreased to near pre-injury levels in WT muscle at these later time points whereas its expression was significantly upregulated in regenerating *Mef2a* KO muscle (Fig. 5D). These results reveal an inverse correlation between *Gtl2-Dio3* miRNA levels and *Sfrp2* expression in regenerating WT and KO muscle, which is coordinately dysregulated in *Mef2a* KO mice.

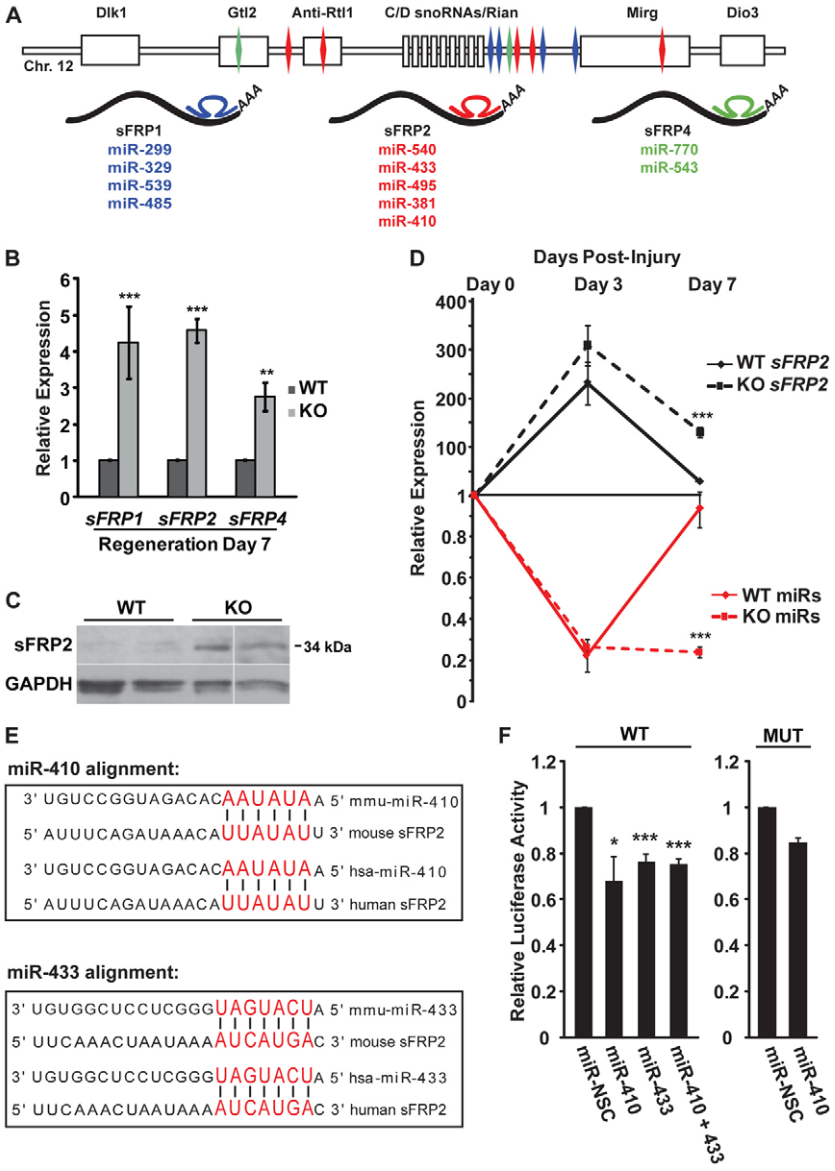

Fig. 5. *Gtl2-Dio3* miRNAs directly regulate the 3′UTR of *Sfrp2*. (**A**) Schematic of miRs (colored diamonds) predicted to target the 3′UTRs of *Sfrp1*, *Sfrp2* and *Sfrp4* (MirANDA). Grouped miRNAs under each *Sfrp* transcript, listed from top to bottom, reflects their 5′ to 3′ order within the *Gtl2-Dio3* locus. (**B**) *Sfrp* expression in WT and KO TA muscle, 7 days post-injury (n=3). (**C**) sFRP2 protein expression in WT and KO TA muscle, 7 days post-injury (n=2). Space indicates non-adjacent lanes from one blot. (**D**) miRNA and *Sfrp2* changes in gene expression during regeneration. miR expression values represent the average change in gene expression of five miRs (miR-540-3p, miR-433, miR-495, miR-381, miR-410) predicted to target the 3′UTR of *Sfrp2* (n=3). At regeneration day 7, *Sfrp2* levels in *Mef2a* KO mice are 4.5-fold higher than WT. At this timepoint, WT *Sfrp2* levels are 27-fold higher than pre-injury levels. (**E**) Sequence alignments of miR-410 and miR-433 seed sequences and predicted 3′UTR *sFRP2* target sites (MirANDA). (**F**) Luciferase analysis of pMIR-REPORT-3′UTR-*sFRP2* (WT) and the miR-410 seed sequence mutant (MUT), co-transfected with miR-410 and miR-433 precursor miRNA mimics (150 nM, Ambion) in COS cells compared with a non-specific control (NSC) miR mimic (n=6). Error bars represent s.e.m. *P<0.05, **P<0.01, ***P<0.001.

miRNAs in the *Gtl2-Dio3* mega-cluster directly regulate 3′UTR of *Sfrp2*

Because many of the miRNAs from the *Gtl2-Dio3* mega-cluster are predicted to target *Sfrp2*, we focused on this gene to determine whether these miRNAs could directly repress its expression. We cloned the 3′UTR of murine *Sfrp2* into the pMIR-REPORT vector (Ambion) and used this construct in transient transfection assays to examine the ability of selected miRNAs to repress this reporter. miRNA mimics (Ambion) were generated for miR-410 (located within *Mirg*) and miR-433 (located within *anti-Rtl1*) because the seed sequences of these miRNAs and their target sequences in *Sfrp2* are absolutely conserved between mouse and human (Fig. 5E). Co-transfection of the *Sfrp2* 3′UTR with either miR-410 or miR-433 mimics resulted in a significant inhibition of the reporter; however, these miRNAs in combination did not inhibit the reporter further (Fig. 5F). Mutation of the miR-410 binding site reduced the ability of miR-410 mimic to repress the reporter (Fig. 5F). These results demonstrate that two miRNAs within the *Gtl2-Dio3* mega-cluster are capable of directly inhibiting *Sfrp2*.

Attenuated WNT activity in *Mef2a*-deficient C2C12 cells and regenerating muscle

Based on the knowledge that sFRPs are inhibitors in the WNT signaling pathway, we would expect that upregulation of sFRP2 in regenerating *Mef2a* KO muscle inhibits WNT activity. To test this possibility, we initially examined *Sfrp* expression and WNT activity in C2C12 cells transduced with sh*Mef2a*. At differentiation day three, we observed a significant upregulation of *Sfrp1*, *Sfrp2* and *Sfrp4*, consistent with our observations in regenerating *Mef2a* KO muscle (Fig. 6A). We then analyzed WNT activity by transfecting *Mef2a*-deficient C2C12 myoblasts with the WNT-sensitive reporter TOPFLASH (Addgene). Luciferase assays revealed an 80% decrease in TOPFLASH activity in sh*Mef2a* transduced cells (Fig. 6B). Supporting these observations, qRT-PCR analysis of endogenous *Axin2*, a WNT-responsive gene (Clevers, 2006), showed a significant 50% decrease in *Mef2a*-deficient C2C12 cells (Fig. 6C).

We next sought to assess WNT activity in regenerating *Mef2a* KO muscle. Translocation of β-catenin from the cytoplasm to the nucleus is one of the major indicators that the WNT signaling

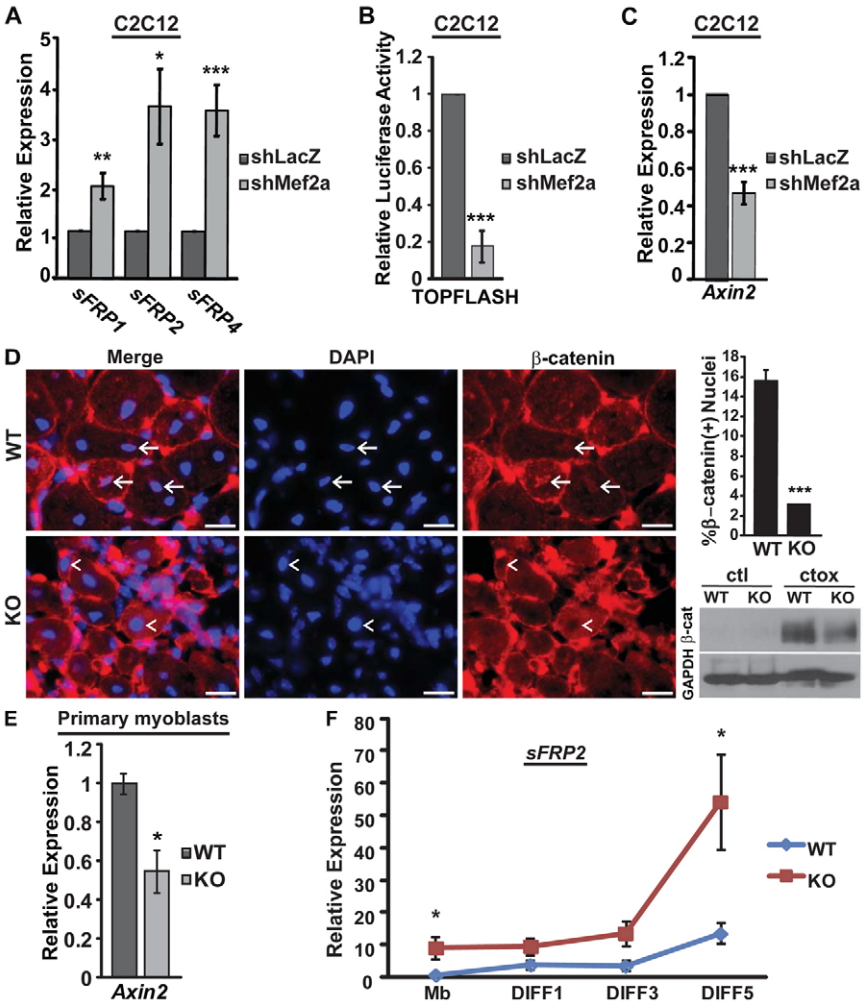

Fig. 6. MEF2A deficiency inhibits WNT signaling. (**A**) *Sfrp* expression in C2C12 DIFF 3 cells transduced with shMef2a. (**B**) Luciferase analysis of the TOPFLASH WNT reporter in C2C12 cells (n=3). (**C**) *Axin2* expression in *Mef2a*-deficient C2C12 cells at DIFF 3 (n=3). (**D**) Immunofluorescence and quantification of β-catenin expression in adult TA muscle, 7 days post-injury. Reduced nuclear β-catenin (arrows) and increased cytoplasmic staining (arrowheads) is evident in KO muscle (n=3). Immunoblot of total β-catenin expression in KO muscle, 7 days post-injury. (**E**) *Axin2* expression in primary myoblasts at DIFF 3 (n=4). (**F**) qRT-PCR analysis of *Sfrp2* expression in primary myoblasts isolated from WT and KO muscle (n=4). Error bars represent s.e.m. *P<0.05, **P<0.01, ***P<0.001. Scale bars: 20 μm.

pathway has been activated (Clevers, 2006; MacDonald et al., 2009). Therefore, we performed immunostaining analysis using a pan β-catenin antibody and found a 75% decrease in β-catenin positive nuclei in *Mef2a* KO regenerating muscle (Fig. 6D) along with an apparent increase in cytoplasmic β-catenin immunoreactivity, suggesting targeting of this protein for proteasomal degradation. Supporting these observations, western blot analysis revealed a reduction in total β-catenin levels in regenerating *Mef2a* KO muscle (Fig. 6D). Moreover, in primary *Mef2a* KO myoblasts isolated from injured muscle *Axin2* expression was reduced (Fig. 6E) and *Sfrp2* was upregulated (Fig. 6F), further demonstrating inhibited WNT activity. Collectively, these results reveal that WNT activity is attenuated in *Mef2a* KO muscle in response to injury, suggesting that this perturbation contributes to impaired myogenic differentiation in this process.

Gtl2-Dio3 miRNAs and recombinant WNTs rescue impaired C2C12 myogenic differentiation

To demonstrate that miRNAs within this mega-cluster are relevant downstream targets of MEF2A in myogenic differentiation, we transfected miRNA mimics into sh*Mef2a*-transduced C2C12 myoblasts. As shown in Fig. 7A, transfection of either miR-410, miR-433, or the two miRs combined was sufficient to rescue the myogenic differentiation defect as demonstrated by increased myotube formation and myosin heavy chain (MHC) expression. We then assessed rescue of WNT activity by way of *Axin2* expression, and observed that *Axin2* was restored to equal to or greater than control levels in the presence of the miRNA mimics individually or in combination (Fig. 7B). Furthermore, transfection of C2C12 myoblasts with inhibitors (anti-miRs) of miR-410 and miR-433 resulted in impaired myogenesis (Fig. 7C) supporting the notion that their downregulation plays a role in the differentiation defect in *Mef2a*-deficient myoblasts. Finally, if reduced WNT activity is also contributing to impaired myogenesis in *Mef2a*-deficient myoblasts then activating this pathway would be expected to properly restore differentiation. Treatment of *Mef2a*-deficient C2C12 myoblasts with recombinant WNT3A or WNT5A effectively rescued differentiation (Fig. 7D). These data demonstrate that the *Gtl2-Dio3* miRNAs function downstream of MEF2A to modulate WNT signaling in myogenic differentiation.

DISCUSSION

The results of this study reveal an essential role for MEF2A in skeletal muscle regeneration. Our data demonstrate that regenerating myoblasts initiate a gene program that is distinct from that occurring during development and is characterized by the early expression of MEF2A. Accordingly, skeletal muscle lacking MEF2A is unable to regenerate properly in response to injury. We show that MEF2A functions in regenerative myogenesis by regulating transcription of the *Gtl2-Dio3* miRNA mega-cluster and that several of these miRNAs target sFRP2, an inhibitor of WNT

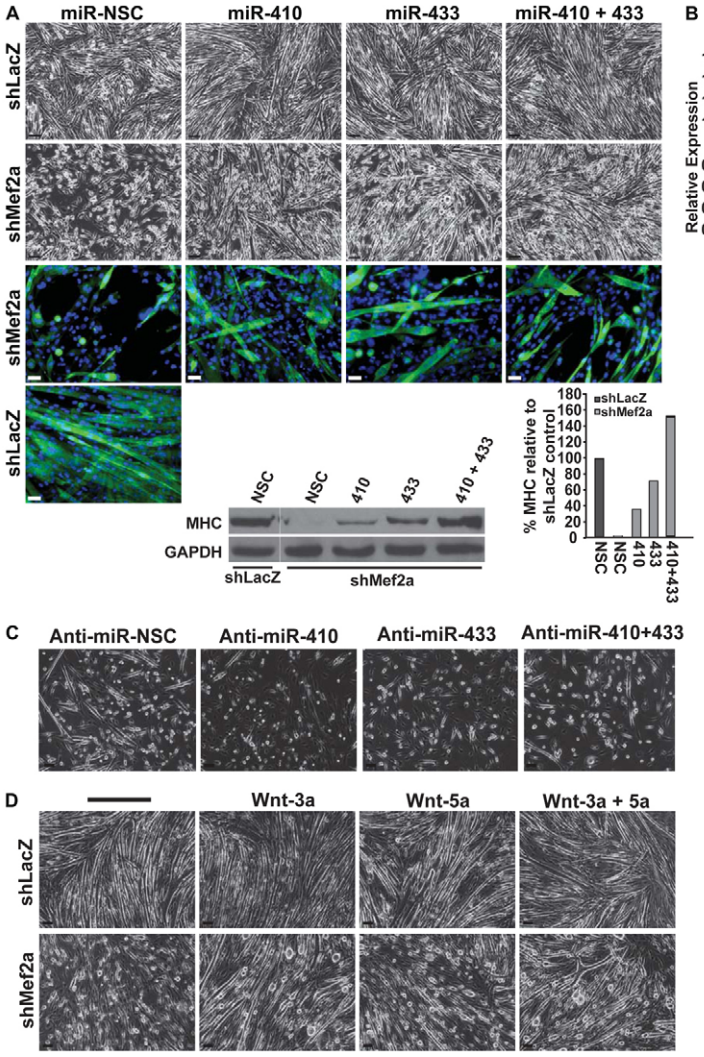

Fig. 7. *Gtl2-Dio3* miRNAs and recombinant WNTs rescue the *Mef2A*-deficient myogenic differentiation defect. (**A**) Phase contrast images (upper panels), α-actinin immunofluorescence (lower panels) and MHC immunoblot of C2C12 DIFF 3 cells transduced with sh*lacZ* or sh*Mef2a*, and transfected with 40 nM miR-410, miR-433 or miR-NSC mimics (n=3). Results demonstrate rescue of myogenic differentiation. (**B**) qRT-PCR analysis of *Axin2* expression for miR rescue experiments shown in A. (**C**) Phase contrast images of C2C12 DIFF 3 cells transfected with anti-miR-NSC, anti-miR410, anti-miR-433, or anti-miRs 410 and 433 combined reveal impaired myotube formation. (**D**) Phase contrast images of C2C12 DIFF 3 cells transduced with sh*lacZ* or sh*Mef2a* and treated with recombinant mouse WNT3A, WNT5A, or both WNTs combined. NSC, non-specific control. Error bars represent s.e.m. *P<0.05, **P<0.01, ***P<0.001. Scale bars: 20 μm.

signaling. Consistent with these observations, injured *Mef2a* KO muscle exhibits increased sFRP expression and attenuated WNT activity. These results firmly establish a molecular link between two important developmental regulators, MEF2 and WNT, in the process of adult regenerative myogenesis. To our knowledge, this is the first evidence that MEF2 participates in the regulation of WNT signaling.

Previous studies on *Mef2a* KO mice concluded that this factor is largely dispensable in skeletal muscle development (Potthoff et al., 2007b). By contrast, the present study shows that MEF2A is essential for skeletal muscle regeneration. These observations suggest that MEF2A activity is regulated in a context-dependent manner, i.e. embryonic versus adult muscle. Alternatively, the skeletal muscle regeneration defect might reflect differences in the temporal expression of *Mef2a*. In embryonic muscle development, *Mef2a* is expressed after *Mef2b* and *Mef2c* (Edmondson et al., 1994). But in activated, primary and C2C12 myoblasts *Mef2a* is one of the earliest *Mef2* genes expressed with transcripts detectable prior to *Mef2c* induction, which is consistent with this factor playing an essential role in myoblast differentiation (this study) (Seok et al., 2011). Moreover, upon injury, expression of *Mef2a* is upregulated (supplementary material Fig. S1C and Fig. S3B), whereas *Mef2c* is downregulated in regenerating muscle (Zhao and Hoffman, 2004). Although it remains to be determined whether other MEF2 family members function in skeletal muscle regeneration, our data suggest that the regulation and/or activity of MEF2A has been reprogrammed such that it plays a more prominent role in adult myogenesis. This notion is supported by a recent report demonstrating co-expression of MEF2 and MyoD in activated satellite cells in regenerating muscle (Mokalled et al., 2012).

Muscle injury in adult mice triggers the activation of quiescent PAX7+ satellite cells, which proliferate as muscle progenitors (myoblasts) and subsequently differentiate into myotubes (Zammit et al., 2004; Olguin and Olwin, 2004; Chargé and Rudnicki, 2004; Zammit, 2008). We noted a significant reduction in PAX7+ nuclei and expression in injured *Mef2a* KO muscle, suggesting that mutant muscle is unable to maintain or generate the appropriate number of activated progenitors resulting in impaired myogenesis with smaller, immature myofibers. These results suggest that MEF2A functions upstream of or in parallel to PAX7 in muscle progenitors, though a definitive answer will require detailed characterization of sorted myoblasts from mutant tissue. Alternatively, the depletion in PAX7+ nuclei could be linked to a downstream differentiation function of MEF2A in the muscle regeneration process. That is, regenerating nascent or mature myotubes lacking MEF2A are unable to properly communicate with the injured microenvironment thereby

adversely affecting the muscle progenitor population. Based on the established role of MEF2 proteins in muscle differentiation this latter notion appears to be the most plausible interpretation of the PAX7 deficiency. Our findings that PAX7 expression is not significantly reduced in *Mef2a* KO muscle until day 3 post-injury or in mutant primary myoblasts until the onset of differentiation (day 1) support this hypothesis.

The delay in regeneration suggests that other factors or pathways are ultimately able to compensate for the loss of MEF2A. One obvious explanation is that the remaining MEF2 proteins are partially functionally redundant with MEF2A and are less effective regulators of MEF2A-dependent gene programs in the muscle regeneration process. Because we used a global *Mef2a* KO it is also possible that the lack of MEF2A in non-muscle cells, such as inflammatory cells, contributes to the regeneration defect and delay in myofiber formation. In particular, the observation that injured *Mef2a* KO muscle eventually recovers suggests that inefficient clearance of necrotic myofibers, which is associated with the immune response, is an integral part of the phenotype.

Our studies also reveal that the WNT signal transduction cascade is modulated by MEF2A in skeletal muscle regeneration. WNT signaling has been established as an important regulator in adult regenerative myogenesis yet the mechanisms by which this pathway is modulated remain incompletely understood. WNT signaling in regeneration is complex and has been reported to be required for satellite cell proliferation, self-renewal and differentiation (Polesskaya et al., 2003; Brack et al., 2008; Otto et al., 2008). Given the diverse roles of WNT, the activity of this pathway would need to be tightly controlled throughout adult myogenesis in order to maintain a balance between proliferating, activated progenitors and myoblasts committed to differentiation. We show that defective regenerative myogenesis in *Mef2a* KO muscle is associated with aberrant WNT signaling. The WNT reporter and target gene expression assays performed with *Mef2a*-deficient primary myoblasts and C2C12 cells reveal reduced WNT activity in differentiated myotubes and suggest that it impacts this myogenic process, resulting in impaired myofiber formation. This notion is reinforced by the observation that treatment of *Mef2a*-deficient C2C12 cells with recombinant WNTs rescued myotube differentiation. However, as stated above, the reduction in PAX7+ nuclei and PAX7 expression *in vivo* implies that the depletion of activated progenitors also contributes to diminished myofiber formation. Although it is presently unclear whether inadequate proliferation or reduced viability of these myogenic progenitors is the reason for the depletion, the reduction in this progenitor population can also be attributable to attenuated WNT activity. Conceivably, WNT signaling might be acting on both the maturation of myotubes and undifferentiated, proliferating myoblasts. Because WNT signaling in regenerative myogenesis has pleiotropic effects it is likely that various cellular decisions are affected in this mutant.

MEF2A functions in regeneration by controlling transcription of the *Gtl2-Dio3* miRNA locus. The *Gtl2-Dio3* domain is the largest known non-coding RNA cluster in mammals and contains >40 miRNAs (Seitz et al., 2004; Kircher et al., 2008). Previous studies have suggested that transcription of miRNA sub-clusters within the *Gtl2-Dio3* locus is regulated by different promoters (Song and Wang, 2008; Fiore et al., 2009). Although the aforementioned studies suggest the presence of independent *cis*-acting sequences within the *Gtl2-Dio3* locus, our data support the notion that the *Gtl2-Dio3* mega-cluster is coordinately regulated by an upstream MEF2A-dependent promoter. This rationale is based on two observations. First, a mouse knockout of the *Gtl2* proximal promoter, which harbors the MEF2 binding site, results in downregulation of miRNAs in the *Gtl2-Dio3* cluster with associated developmental skeletal muscle defects (Zhou et al., 2010). Second, we show that the tissue expression pattern of multiple miRNAs distributed throughout the cluster is similar, and that they are all downregulated in regenerating *Mef2a* knockout muscle. Although it is possible that sub-clusters of miRNAs within the *Gtl2-Dio3* domain are differentially regulated by independent *cis*-acting sequences, the most logical explanation for the widespread, coordinated downregulation of this cluster in our and other models is through a single upstream control element. It remains to be determined whether the *Gtl2-Dio3* mega-cluster is transcribed as a single, large polycistronic primary RNA transcript.

Given the connection of the MEF2A/*Gtl2-Dio3* miRNA pathway to regeneration, it is tempting to speculate that this genetic pathway also plays an important role in muscular dystrophies. It is known that many muscular dystrophies are characterized by continuous cycles of degeneration and regeneration, ultimately resulting in failure to form new myofibers because muscle progenitors have been exhausted in this process (Wallace and McNally, 2009). Recently, it was reported that expression and splicing of MEF2A is dysregulated in various muscular dystrophies (Bachinski et al., 2010). Perhaps these and other muscle dystrophies might be associated with perturbed *Gtl2-Dio3* miRNA expression resulting from altered MEF2A regulation. Indeed, numerous miRNAs are dysregulated in several muscular dystrophies (Eisenberg et al., 2007) and we have found that some of these map to the *Gtl2-Dio3* locus. Our findings point to the importance of interrogating further MEF2A function in muscle diseases involving impaired muscle regeneration, and represent an attractive area of investigation for degenerative muscle disorders.

Acknowledgements
We thank Ning Liu and Eric Olson (UT Southwestern) and Dazhi Wang (Children's Hospital, Boston) for sharing unpublished miRNA data. We also thank David Goldhamer (University of Connecticut) for providing us with a Pax7 immunostaining protocol and Tod Gulick (Sanford Burnham Institute) for the MEF2-FLAG expression constructs. We are grateful to Kim McCall, Tom Gilmore and Isabel Dominguez at Boston University for providing us with additional reagents and advice.

Funding
This work was supported by a grant from the National Institutes of Health National Heart, Lung, and Blood Institute [HL73304 to F.J.N.]. Deposited in PMC for release after 12 months.

Competing interests statement
The authors declare no competing financial interests.

Supplementary material
Supplementary material available online at
http://dev.biologists.org/lookup/suppl/doi:10.1242/dev.081851/-/DC1

References

Bachinski, L. L., Sirito, M., Böhme, M., Baggerly, K. A., Udd, B. and Krahe, R. (2010). Altered MEF2 isoforms in myotonic dystrophy and other neuromuscular disorders. *Muscle Nerve* **42**, 856-863.
Bartel, D. P. (2004). MicroRNAs: genomics, biogenesis, mechanism, and function. *Cell* **116**, 281-297.
Black, B. L. and Olson, E. N. (1998). Transcriptional control of muscle development by myocyte enhancer factor-2 (MEF2) proteins. *Annu. Rev. Cell Dev. Biol.* **14**, 167-196.
Blau, H. M., Chiu, C. P. and Webster, C. (1983). Cytoplasmic activation of human nuclear genes in stable heterocaryons. *Cell* **32**, 1171-1180.
Bour, B. A., O'Brien, M. A., Lockwood, W. L., Goldstein, E. S., Bodmer, R., Taghert, P. H., Abmayr, S. M. and Nguyen, H. T. (1995). *Drosophila* MEF2, a transcription factor that is essential for myogenesis. *Genes Dev.* **9**, 730-741.

Brack, A. S., Conboy, I. M., Conboy, M. J., Shen, J. and Rando, T. A. (2008). A temporal switch from notch to Wnt signaling in muscle stem cells is necessary for normal adult myogenesis. *Cell Stem Cell* **2**, 50-59.
Buckingham, M. (2006). Myogenic progenitor cells and skeletal myogenesis in vertebrates. *Curr. Opin. Genet. Dev.* **16**, 525-532.
Buckingham, M. and Relaix, F. (2007). The role of Pax genes in the development of tissues and organs: Pax3 and Pax7 regulate muscle progenitor cell functions. *Annu. Rev. Cell Dev. Biol.* **23**, 645-673.
Chargé, S. B. and Rudnicki, M. A. (2004). Cellular and molecular regulation of muscle regeneration. *Physiol. Rev.* **84**, 209-238.
Chen, C., Ridzon, D. A., Broomer, A. J., Zhou, Z., Lee, D. H., Nguyen, J. T., Barbisin, M., Xu, N. L., Mahuvakar, V. R., Andersen, M. R. et al. (2005). Real-time quantification of microRNAs by stem-loop RT-PCR. *Nucleic Acids Res.* **33**, e179.
Chen, J. F., Mandel, E. M., Thomson, J. M., Wu, Q., Callis, T. E., Hammond, S. M., Conlon, F. L. and Wang, D. Z. (2006). The role of microRNA-1 and microRNA-133 in skeletal muscle proliferation and differentiation. *Nat. Genet.* **38**, 228-233.
Chen, J. F., Callis, T. E. and Wang, D. Z. (2009). microRNAs and muscle disorders. *J. Cell Sci.* **122**, 13-20.
Chen, J. F., Tao, Y., Li, J., Deng, Z., Yan, Z., Xiao, X. and Wang, D. Z. (2010). microRNA-1 and microRNA-206 regulate skeletal muscle satellite cell proliferation and differentiation by repressing Pax7. *J. Cell Biol.* **190**, 867-879.
Clevers, H. (2006). Wnt/beta-catenin signaling in development and disease. *Cell* **127**, 469-480.
Crist, C. G., Montarras, D., Pallafacchina, G., Rocancourt, D., Cumano, A., Conway, S. J. and Buckingham, M. (2009). Muscle stem cell behavior is modified by microRNA-27 regulation of Pax3 expression. *Proc. Natl. Acad. Sci. USA* **106**, 13383-13387.
Edmondson, D. G., Lyons, G. E., Martin, J. F. and Olson, E. N. (1994). Mef2 gene expression marks the cardiac and skeletal muscle lineages during mouse embryogenesis. *Development* **120**, 1251-1263.
Eisenberg, I., Eran, A., Nishino, I., Moggio, M., Lamperti, C., Amato, A. A., Lidov, H. G., Kang, P. B., North, K. N., Mitrani-Rosenbaum, S. et al. (2007). Distinctive patterns of microRNA expression in primary muscular disorders. *Proc. Natl. Acad. Sci. USA* **104**, 17016-17021.
Ewen, E. P., Snyder, C. M., Wilson, M., Desjardins, D. and Naya, F. J. (2011). The Mef2A transcription factor coordinately regulates a costamere gene program in cardiac muscle. *J. Biol. Chem.* **286**, 29644-29653.
Fiore, R., Khudayberdiev, S., Christensen, M., Siegel, G., Flavell, S. W., Kim, T. K., Greenberg, M. E. and Schratt, G. (2009). Mef2-mediated transcription of the miR379-410 cluster regulates activity-dependent dendritogenesis by fine-tuning Pumilio2 protein levels. *EMBO J.* **28**, 697-710.
Kanisicak, O., Mendez, J. J., Yamamoto, S., Yamamoto, M. and Goldhamer, D. J. (2009). Progenitors of skeletal muscle satellite cells express the muscle determination gene, *MyoD*. *Dev. Biol.* **332**, 131-141.
Kawano, Y. and Kypta, R. (2003). Secreted antagonists of the Wnt signalling pathway. *J. Cell Sci.* **116**, 2627-2634.
Kircher, M., Bock, C. and Paulsen, M. (2008). Structural conservation versus functional divergence of maternally expressed microRNAs in the *Dlk1/Gtl2* imprinting region. *BMC Genomics* **9**, 346-364.
Kuang, S. and Rudnicki, M. A. (2008). The emerging biology of satellite cells and their therapeutic potential. *Trends Mol. Med.* **14**, 82-91.
Kuang, S., Chargé, S. B., Seale, P., Huh, M. and Rudnicki, M. A. (2006). Distinct roles for Pax7 and Pax3 in adult regenerative myogenesis. *J. Cell Biol.* **172**, 103-113.
Lagos-Quintana, M., Rauhut, R., Yalcin, A., Meyer, J., Lendeckel, W. and Tuschl, T. (2002). Identification of tissue-specific microRNAs from mouse. *Curr. Biol.* **12**, 735-739.
Lepper, C., Conway, S. J. and Fan, C. M. (2009). Adult satellite cells and embryonic muscle progenitors have distinct genetic requirements. *Nature* **460**, 627-631.
Lilly, B., Zhao, B., Ranganayakulu, G., Paterson, B. M., Schulz, R. A. and Olson, E. N. (1995). Requirement of MADS domain transcription factor D-MEF2 for muscle formation in *Drosophila*. *Science* **267**, 688-693.
Lin, S. P., Youngson, N., Takada, S., Seitz, H., Reik, W., Paulsen, M., Cavaille, J. and Ferguson-Smith, A. C. (2003). Asymmetric regulation of imprinting on the maternal and paternal chromosomes at the Dlk1-Gtl2 imprinted cluster on mouse chromosome 12. *Nat. Genet.* **35**, 97-102.
Liu, N., Williams, A. H., Kim, Y., McAnally, J., Bezprozvannaya, S., Sutherland, L. B., Richardson, J. A., Bassel-Duby, R. and Olson, E. N. (2007). An intragenic MEF2-dependent enhancer directs muscle-specific expression of microRNAs 1 and 133. *Proc. Natl. Acad. Sci. USA* **104**, 20844-20849.
MacDonald, B. T., Tamai, K. and He, X. (2009). Wnt/β-catenin signaling: components, mechanisms, and diseases. *Dev. Cell* **17**, 9-26.
McCalmon, S. A., Desjardins, D. M., Ahmad, S., Davidoff, K. S., Snyder, C. M., Sato, K., Ohashi, K., Kielbasa, O. M., Mathew, M., Ewen, E. P. et al. (2010). Modulation of angiotensin II-mediated cardiac remodeling by the MEF2A target gene Xirp2. *Circ. Res.* **106**, 952-960.
Miller, J. M., ed. (1972). Assay for β-galactosidase. In *Molecular Genetics*, pp. 352-355. Cold Spring Harbor, New York: Cold Spring Harbor Laboratory Press.
Mokalled, M. H., Johnson, A. N., Creemers, E. E. and Olson, E. N. (2012). MASTR directs MyoD-dependent satellite cell differentiation during skeletal muscle regeneration. *Genes Dev.* **26**, 190-202.
Naya, F. J., Black, B. L., Wu, H., Bassel-Duby, R., Richardson, J. A., Hill, J. A. and Olson, E. N. (2002). Mitochondrial deficiency and cardiac sudden death in mice lacking the MEF2A transcription factor. *Nat. Med.* **8**, 1303-1309.
Olguin, H. C. and Olwin, B. B. (2004). Pax-7 up-regulation inhibits myogenesis and cell cycle progression in satellite cells: a potential mechanism for self-renewal. *Dev. Biol.* **275**, 375-388.
Otto, A., Schmidt, C., Luke, G., Allen, S., Valasek, P., Muntoni, F., Lawrence-Watt, D. and Patel, K. (2008). Canonical Wnt signalling induces satellite-cell proliferation during adult skeletal muscle regeneration. *J. Cell Sci.* **121**, 2939-2950.
Parker, M. H., Seale, P. and Rudnicki, M. A. (2003). Looking back to the embryo: defining transcriptional networks in adult myogenesis. *Nat. Rev. Genet.* **4**, 497-507.
Polesskaya, A., Seale, P. and Rudnicki, M. A. (2003). Wnt signaling induces the myogenic specification of resident CD45+ adult stem cells during muscle regeneration. *Cell* **113**, 841-852.
Potthoff, M. J. and Olson, E. N. (2007). MEF2: a central regulator of diverse developmental programs. *Development* **134**, 4131-4140.
Potthoff, M. J., Arnold, M. A., McAnally, J., Richardson, J. A., Bassel-Duby, R. and Olson, E. N. (2007a). Regulation of skeletal muscle sarcomere integrity and postnatal muscle function by *Mef2c*. *Mol. Cell. Biol.* **27**, 8143-8151.
Potthoff, M. J., Wu, H., Arnold, M. A., Shelton, J. M., Backs, J., McAnally, J., Richardson, J. A., Bassel-Duby, R. and Olson, E. N. (2007b). Histone deacetylase degradation and MEF2 activation promote the formation of slow-twitch myofibers. *J. Clin. Invest.* **117**, 2459-2467.
Schratt, G. M., Tuebing, F., Nigh, E. A., Kane, C. G., Sabatini, M. E., Kiebler, M. and Greenberg, M. E. (2006). A brain-specific microRNA regulates dendritic spine development. *Nature* **439**, 283-289.
Seitz, H., Royo, H., Bortolin, M. L., Lin, S. P., Ferguson-Smith, A. C. and Cavaillé, J. (2004). A large imprinted microRNA gene cluster at the mouse Dlk1-Gtl2 domain. *Genome Res.* **14**, 1741-1748.
Seok, H. Y., Tatsuguchi, M., Callis, T. E., He, A., Pu, W. T. and Wang, D. Z. (2011). miR-155 inhibits expression of the MEF2A protein to repress skeletal muscle differentiation. *J. Biol. Chem.* **286**, 35339-35346.
Shi, X. and Garry, D. J. (2006). Muscle stem cells in development, regeneration, and disease. *Genes Dev.* **20**, 1692-1708.
Song, G. and Wang, L. (2008). MiR-433 and miR-127 arise from independent overlapping primary transcripts encoded by the miR-433-127 locus. *PLoS ONE* **3**, e3574-e3578.
Springer, M. L., Rando, T. and Blau, H. M. (1997). Gene delivery to muscle. In *Current Protocols in Human Genetics*. New York, NY: John Wiley & Sons.
Tajbakhsh, S. (2009). Skeletal muscle stem cells in developmental versus regenerative myogenesis. *J. Intern. Med.* **266**, 372-389.
Tedesco, F. S., Dellavalle, A., Diaz-Manera, J., Messina, G. and Cossu, G. (2010). Repairing skeletal muscle: regenerative potential of skeletal muscle stem cells. *J. Clin. Invest.* **120**, 11-19.
Thompson, R. C., Herscovitch, M., Zhao, I., Ford, T. J. and Gilmore, T. D. (2011). NF-kappaB down-regulates expression of the B-lymphoma marker CD10 through a miR-155/PU.1 pathway. *J. Biol. Chem.* **286**, 1675-1682.
van Rooij, E., Liu, N. and Olson, E. N. (2008). MicroRNAs flex their muscles. *Trends Genet.* **24**, 159-166.
Waddell, J. N., Zhang, P., Wen, Y., Gupta, S. K., Yevtodiyenko, A., Schmidt, J. V., Bidwell, C. A., Kumar, A. and Kuang, S. (2010). Dlk1 is necessary for proper skeletal muscle development and regeneration. *PLoS ONE* **5**, e15055.
Wallace, G. Q., and McNally, E. M. (2009). Mechanisms of muscle degeneration, regeneration, and repair in the muscular dystrophies. *Annu. Rev. Physiol.* **71**, 7.1-7.21.
Yaffe, D. and Saxel, O. (1977). Serial passaging and differentiation of myogenic cells isolated from dystrophic mouse muscle. *Nature* **270**, 725-727.
Zammit, P. S. (2008). All muscle satellite cells are equal, but are some more equal than others? *J. Cell Sci.* **121**, 2975-2982.
Zammit, P. S., Golding, J. P., Nagata, Y., Hudon, V., Partridge, T. A. and Beauchamp, J. R. (2004). Muscle satellite cells adopt divergent fates: a mechanism for self-renewal? *J. Cell Biol.* **166**, 347-357.
Zhao, P. and Hoffman, E. P. (2004). Embryonic myogenesis pathways in muscle regeneration. *Dev. Dyn.* **229**, 380-392.
Zhou, Y., Cheunsuchon, P., Nakayama, Y., Lawlor, M. W., Zhong, Y., Rice, K. A., Zhang, L., Zhang, X., Gordon, F. E., Lidov, H. G. et al. (2010). Activation of paternally expressed genes and perinatal death caused by deletion of the *Gtl2* gene. *Development* **137**, 2643-2652.

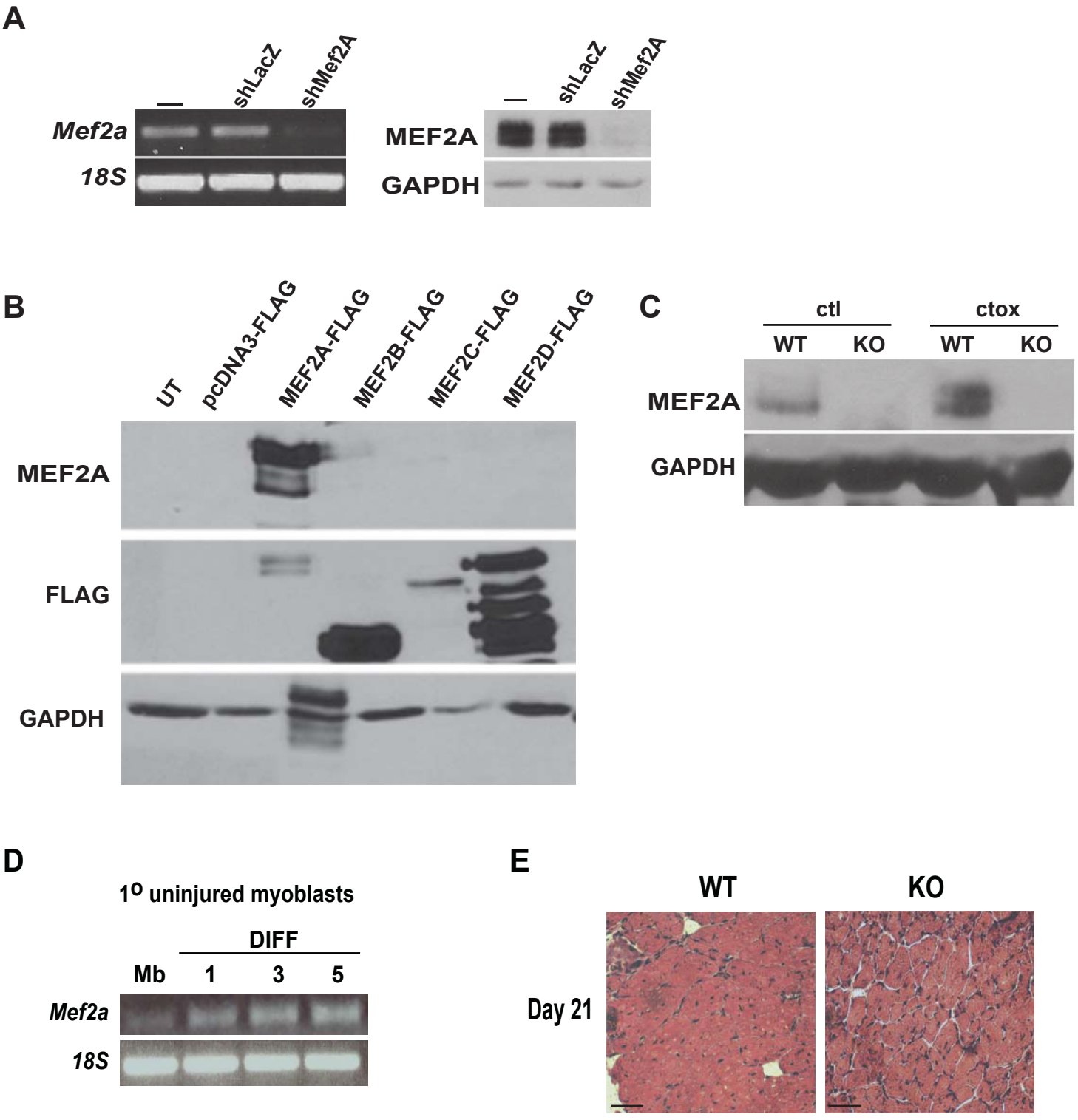

Fig. S1. Antibody and shRNA specificity for MEF2A and MEF2A expression in regeneration. (**A**) RT-PCR (left) and western blot (right) analysis of C2C12 DIFF3, post-transduction with sh*lacZ* or sh*Mef2a*. 18S rRNA and GAPDH are loading controls. (**B**) Immunoblot of MEF2-FLAG expression in COS cells with the MEF2A antibody (C-21, Santa Cruz). GAPDH is the loading control. (**C**) Immunoblot of MEF2A expression in uninjured (ctl) and injured (ctox, day 7) skeletal muscle from WT and Mef2a KO mice. (**D**) RT-PCR analysis of *Mef2a* expression in differentiation using uninjured primary myoblasts. (**E**) Hematoxylin and Eosin staining of transverse TA muscle sections at day 21 post-injury. Data reveals substantially improved myofiber formation in regenerating *Mef2a* KO.

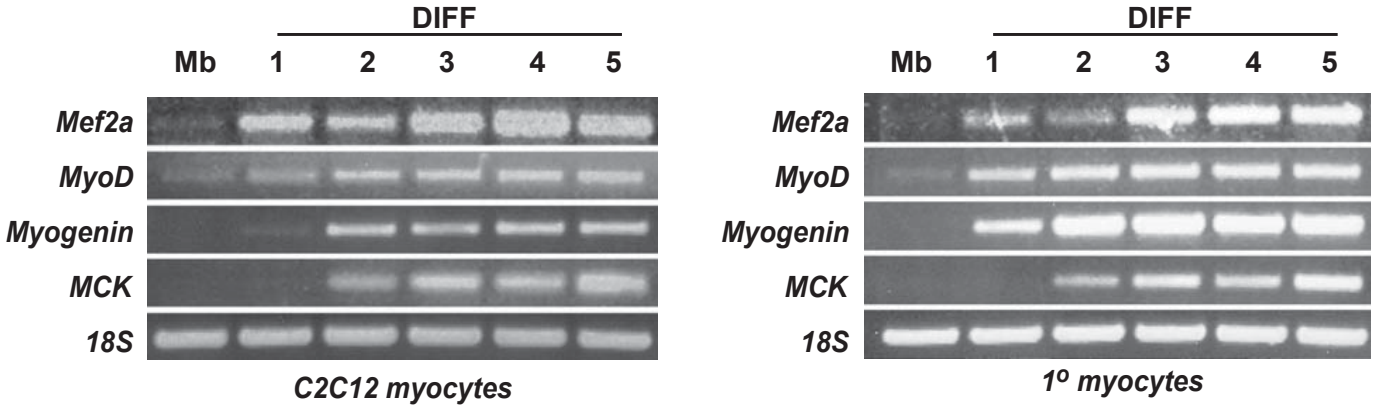

Fig. S2. C2C12 differentiation mimics regenerating primary myocytes. RT-PCR time course of myogenic marker expression during differentiation, myoblasts (Mb) through DIFF 5, in C2C12 cells and primary WT myocytes.

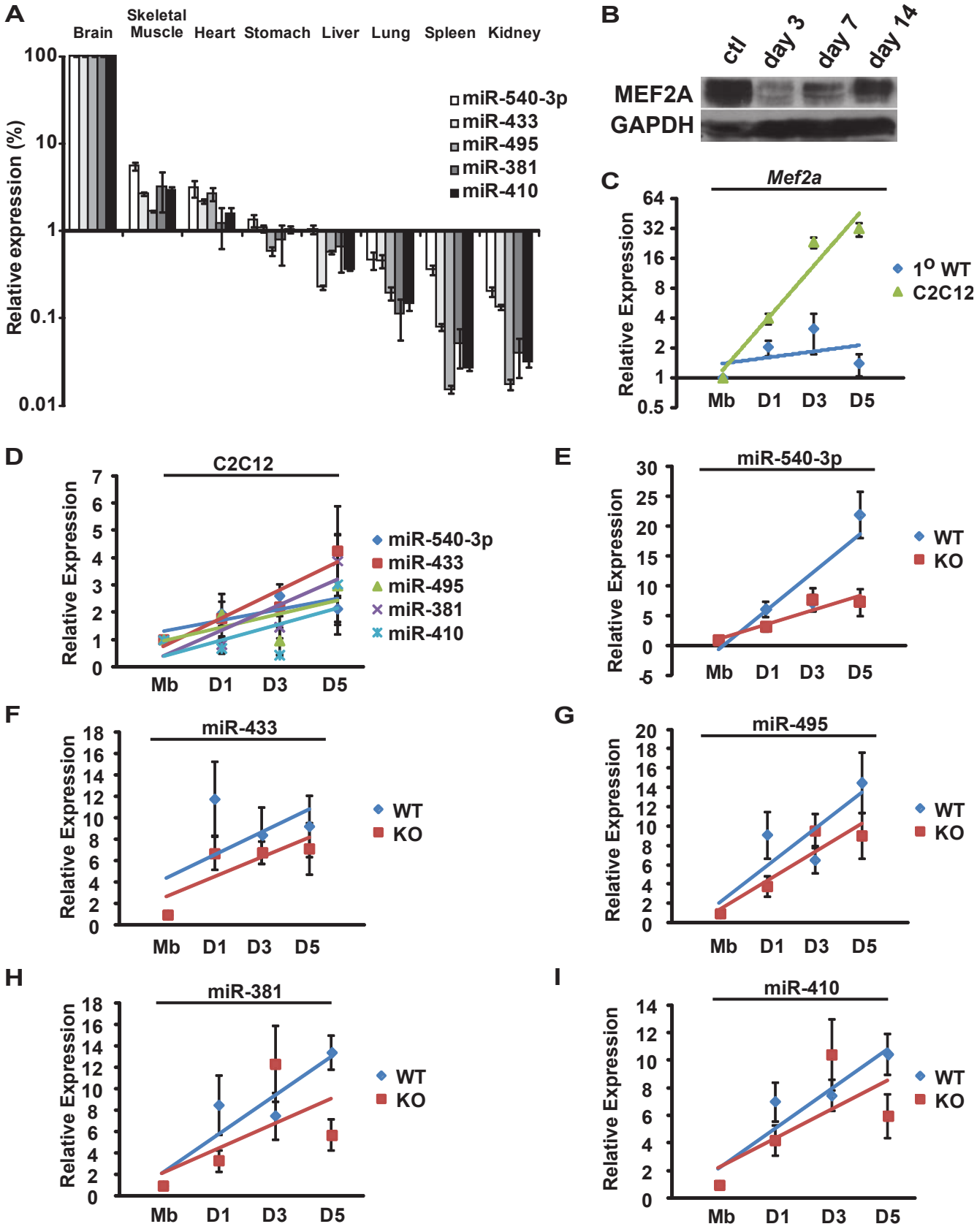

Fig. S3. miR expression patterns mimic MEF2A. (**A**) Expression of selected miRNAs in various tissues are displayed relative to the brain (normalized to 100%) (*n*=3). (**B**) Immunoblot of MEF2A expression in control (ctl) and regenerating muscle (days 3-14). (**C**) Mef2a expression in primary WT myocytes and C2C12 cells during differentiation. (**D**) miR expression in C2C12 cells during differentiation. (**E-I**) Expression of individual miRs in WT and *Mef2a* KO primary myocytes during differentiation. Myoblast (Mb) and DIFF 1-5 (D1-D5) time points are indicated. Changes in expression are displayed as linear trendlines. Error bars represent s.e.m.

RT-PCR

Oligo	Direction	Sequence 5' to 3'
18SrRNA	Forward	CATTCGAACGTCTGCCCTAT
	Reverse	CCTCCAATGGATCCTCGTTA
Mef2a	Forward	ACACGCATAATGGATGAGAGGAACCGAC
	Reverse	CAACGATATCCGAGTTCGTCCTGCTTTC
Mef2b	Forward	GAAAGAAAGCCGCTCTGCACAG
	Reverse	ACCTCTGGCCCCTCCTCCATA
Mef2c	Forward	CAGGGACGAGAGAGAGAAGAAAC
	Reverse	CAATCTTTGCCTGCTGATCATTAG
Mef2d	Forward	CTTTCCTCTCTGGCACTAAGGAC
	Reverse	CCAGTCTATAACTCTGCATCATC
MyoD	Forward	TCGAAGGTCTGCAGGCTCTGC
	Reverse	TGCAGTCGATCTCTCAAAGCACC
Myogenin	Forward	TGGAGCTGTATGAGACATCCC
	Reverse	GAGTTGCATTCACTGGGCAC
MCK	Forward	CTGACCCCTGACCTCTACAAT
	Reverse	CATGGCGGTCCTGGATGAT

qRT-PCR

Oligo	Direction	Sequence 5' to 3'
GAPDH	Forward	TGGCAAAGTGGAGATTGTTGCC
	Reverse	AAGATGGTGATGGGCTTCCCG
Dlk1	Forward	AGTGCGAAACCTGGGTGTC
	Reverse	GCCTCCTTGTTGAAAGTGGTCA
Gtl2	Forward	TGGAATAGGCCAACATCGTCA
	Reverse	AGGCTCTGTGTCCATGTGTCC
pre-miR-127	Forward	TTTGATCACTGTCTCCAGCCTGCTG
	Reverse	GATGATGAGACTTCCGACCAGCCA
sFRP1	Forward	CAACGTGGGCTACAAGAAGAT
	Reverse	GGCCAGTAGAAGCCGAAGAAC
sFRP2	Forward	CCCCTGTCTGTCTCGACGA
	Reverse	CTTCACACACCTTGGGAGCTT
sFRP4	Forward	AGAAGGTCCATACAGTGGGAAG
	Reverse	GTTACTGCGACTGGTGCGA
Axin2	Forward	TGACTCTCCTTCCAGATCCCA
	Reverse	TGCCCACACTAGGCTGACA
5S rRNA stem loop	Forward	GTTGGCTCTGGTGCAGGGTCCGAGGTATTCGCACCAGAGCCAACAAAGCC
miR 540-3p stem loop	Forward	GTTGGCTCTGGTGCAGGGTCCGAGGTATTCGCACCAGAGCCAACACAGAG
miR 433 stem loop	Forward	GTTGGCTCTGGTGCAGGGTCCGAGGTATTCGCACCAGAGCCAACACACCG
miR 495 stem loop	Forward	GTTGGCTCTGGTGCAGGGTCCGAGGTATTCGCACCAGAGCCAACAAGAAG
miR 381 stem loop	Forward	GTTGGCTCTGGTGCAGGGTCCGAGGTATTCGCACCAGAGCCAACACAGAG
miR 410 stem loop	Forward	GTTGGCTCTGGTGCAGGGTCCGAGGTATTCGCACCAGAGCCAACACAGGC
5SrRNA	Forward	GAATACCGGGTGCTGTAGGC
miR 540-3p	Forward	CAAGGGTCACCCTCTGACTCT
miR 433	Forward	ATCATGATGGGCTCCTCGGT
miR 495	Forward	GCCAAACAAACATGGTGCACTT
miR 381	Forward	GCCTATACAAGGGCAAGCTCTC
miR 410	Forward	CCGCCAATATAACACAGATGGCC
ChIP -39 MEF2	Forward	TCTGGGGGGCTCATTTTTCCG
	Reverse	GAGCCGAGGCGAGCTCTATTC

EMSA

Oligo	Direction	Sequence 5' to 3'
-39 MEF2	Sense	AAGGCTGCGCCTTTATATAAACCCCA
	Antisense	AAGGTGGGGTTTATATAAAGGCGCAG
-39 MUT	Sense	AAGGCTGCGCGGGTATATAAACCCCA
	Antisense	AAGGTGGGGTTTATATACCCGCGCAG

Table S1. Oligonucleotide sequences. Oligonucleotides used for RT-PCR/qRT PCR and EMSA analyses. DNA binding sites in EMSA oligonucleotides are underlined.

Gene Symbol	Fold Change
miR-337	-1.7
miR-540	-1.6
miR-665	-1.3
miR-431	-1.2
miR-341	-1.4
miR 370	-1.3
Rian/MBII-343	-2.1
miR-379	-1.7
miR-411	-1.4
miR-299	-1.6
miR-380	-1.4
miR-329	-1.6
miR-494	-1.3
miR-679	-1.6
miR-666	-1.4
miR-543	-1.7
miR-667	-1.4
miR-376c	-1.2
miR-376b	-1.2
miR-376a	-1.1
miR-300	-1.4
miR-381	-1.5
miR-382	-1.4
miR-134	-1.8
miR-668	-1.3
miR-154	-1.6
miR-496	-1.4
miR-377	-1.5
miR-541	1.0
miR-412	-1.7
miR-369	-1.5

Table S2. MicroRNA expression in injured Mef2a KO muscle. Fold changes in gene expression are presented for additional non-coding RNA transcripts in the *Gtl2-Dio3* locus detected by microarray. Expression values represent fold changes in gene expression between adult *Mef2a* KO cardiotoxin-injured (ctox) and WT ctox muscle tissue samples at regeneration day 7. Non-coding transcripts include microRNAs and the Rian/MBII-343 C/D box sno RNAs and are listed from top to bottom according to their 5′ to 3′ order within the *Gtl2-Dio3* locus.